A Comparative Study on Palmprint Recognition

Hayman Salih Mohammed

Submitted to the
Institute of Graduate Studies and Research
in partial fulfillment of the requirements for the Degree of

Master of Science
in
Computer Engineering

Eastern Mediterranean University
September 2014
Gazimağusa, North Cyprus

Approval of the Institute of Graduate Studies and Research

Prof. Dr. Elvan Yılmaz
Director

I certify that this thesis satisfies the requirements as a thesis for the degree of Master of Science in Computer Engineering.

Prof. Dr. Işık Aybay
Chair, Department of Computer Engineering

We certify that we have read this thesis and that in our opinion it is fully adequate in scope and quality as a thesis for the degree of Master of Science in Computer Engineering.

Asst. Prof. Dr. Önsen Toygar
Supervisor

Examining Committee

1. Asst. Prof. Dr. Yıltan Bitirim
2. Asst. Prof. Dr. Önsen Toygar
3. Asst. Prof. Dr. Ahmet Ünveren

ABSTRACT

Palmprint recognition uses the palm of a person as a biometric for identifying or verifying the human beings. The palmprint contains a number of distinctive features such as principal lines, wrinkles, ridges and minutiae. Therefore, it is appropriate to use feature extraction techniques in order to extract line, texture, statistics and multiple representations.

This thesis presents a comparative study on palmprint recognition using different approaches to extract palmprint features. Appearance-based approaches such as Principal Component Analysis, statistical approaches such as Local Binary Patterns, transform-based approaches such as Discrete Cosine Transform and other approaches such as Log-Gabor filters have been investigated and evaluated on PolyU palmprint database.

The experimental results on both right and left palmprint databases demonstrate that Local Binary Patterns approach is a good texture descriptor which achieves the best recognition accuracy compared to other methods.

Keywords: Log-Gabor, Discrete Cosine Transform, Local Binary Patterns, Principal Component Analysis

ÖZ

Avuçiçi tanıma insanları tanımlamak veya doğrulamak için biyometrik olarak bir kişinin avuçiçini kullanır. Avuçiçi ana hatlar, kırışıklıklar, sırtlar ve önemsiz ayrıntılar gibi bir dizi ayırt edici öznitelikler içerir. Bu nedenle, öznitelik çıkarma tekniklerini kullanarak uygun bir çizgi, doku, istatistik ve çoklu gösterim elde etmek daha uygundur.

Bu tez, avuçiçi özniteliklerini çıkartarak farklı avuçiçi tanıma yaklaşımlarını kıyaslar. Ana Bileşenler Analizi (PCA) gibi görünüm-tabanlı yaklaşımlar, Yerel İkili Örüntü (LBP) gibi doku-tabanlı yaklaşımlar, Ayrık Kosünüs Dönüşümü (DCT) gibi dönüşüm-tabanlı yaklaşımlar ve Log-Gabor filtreleri gibi diğer yaklaşımlar PolyU avuçiçi veritabanı üzerinde incelenmekte ve değerlendirilmektedir.

Hem sağ hem de sol avuçiçi veritabanları üzerinde yapılan deney sonuçları, bize Yerel İkili Örüntü yaklaşımının iyi bir doku tanımlama yöntemi olduğu için diğer yöntemlere göre daha başarılı bir performans elde ettiğini göstermektedir.

Anahtar kelimeler: Log-Gabor, Ayrık Kosünüs Dönüşümü (DCT), Yerel İkili Örüntü (LBP), Ana Bileşenler Analizi (PCA)

Dedicated to my family

ACKNOWLEDGMENT

I would like to start by expressing my gratitude to Asst. Prof. Dr. Önsen Toygar for her guidance as my supervisor. I have learnt a lot from her. She encouraged and pushed me to improve my knowledge and enabled me to be enthusiastic in making this research.

My sincere appreciation also goes to all the professors who tasked out this to give me valuable knowledge in the courses during my studies in Eastern Mediterranean University.

Also, not leaving out my brother, sister and friends who gave me the strength to carry on during my master study.

Finally, special thanks go to my parents who have always been there for me right from my elementary school days till present.

TABLE OF CONTENTS

LIST OF TABLES

LIST OF FIGURES

LIST OF ABBREVIATIONS

LG	Log Gabor
DCT	Discrete Cosine Transform
LBP	Local Binary Patterns
PCA	Principal Component Analysis
GAR	Genuine Acceptance Rate
FAR	False Acceptance Rate
FRR	False Rejection Rate
EER	Equal Error Rate

Chapter 1

INTRODUCTION

The biometrics technology and identification systems have become a principle key for system protection all over the world. By developing new systems and improving the current systems in terms of security, biometric technology has been widely used and significantly played an important role to protect these systems and became a measurable key of protection [1].

The reason of using biometrics in person identification is that each biometric sample is unique and has a stable shape and the features are changing from a person to another. However, human’s eyes cannot see this similarity for some biometrics that includes tiny details and the differences [1]. Moreover, palmprint shape is not changing through the lifetime of a person; newborn palm ridge still maintain with the structure up to death. In addition, each person's palm ridges are not the same even with twins. However, their palms are just similar but not the same [2].

Biometric technology can be categorized into two parts as identification and authentication and it has been applied in many fields and areas such as finger, iris, face and palmprint recognition [3].

In this thesis, palmprint recognition is investigated by applying different feature extraction techniques and the recognition performance for each of them is demonstrated to compare the recognition accuracy of biometrics systems using different feature extraction techniques.

Moreover, there are many difficulties and barriers that are playing an important role in recognition accuracy such as noise and image quality. In addition to these, classification algorithms are playing an important role in increasing the recognition performance.

1.1 System Overview and the Structure

The structure of a palmprint recognition system is like other biometric systems as it is shown in Figure 1.1 [4]. It contains four stages namely image acquisition, preprocessing, feature extraction and classification. The goal for prepressing stage is to enhance the image quality and eliminate the unnecessary parts from the image. After finishing with this stage, the preprocessed image will be sent to feature extraction stage, which is responsible to extract the features of the palm image. Lastly, the image will be sent to the classification stage in order to classify the image samples of the individuals and match the most resembling training image from the image database with the palmprint image used for testing. These stages are explained below in detail.

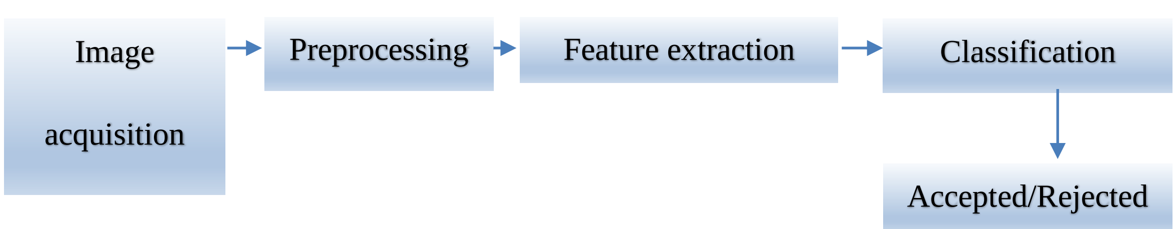

Figure 1.1: Structure of Palmprint Recognition

1.1.1 Image Acquisition

Acquisition is the process of taking image and converting it into matrix data by computer. The image maybe represented as a gray scale image with two dimensions or a color image in three dimensions [5].

1.1.2 Preprocessing

The aim of this stage is preparing images and enhancing them in terms of quality to extract features. It starts by removing the noise of the image to make it clear. The noise typically comes from the degraded functions and unsuitable environments. Moreover, in this stage the images are normalized after getting recovered from the noise [5].

1.1.3 Feature Extraction

This stage is responsible for extracting the necessary lines and ridges, which are required for classification. Extracted features play a big role in the classification step. The small lines and ridges are important to get images recognized in the classification step [5].

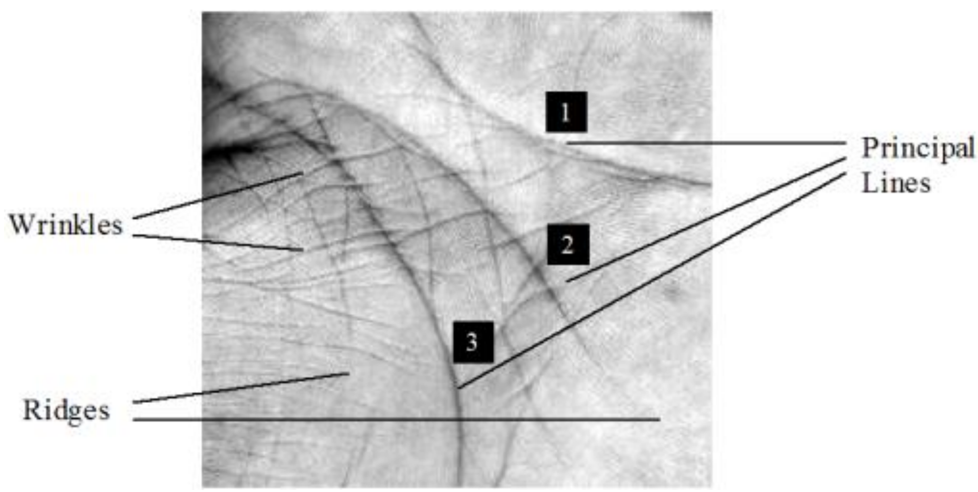

Figure 1.2: A Sample of Palmprint Image With Defined Lines [6]

The most important feature of the palm pattern is a line characteristic, as it is shown in Figure 1.2 [6]. These lines can be divided into two or three main groups such as wrinkles, ridges and principal lines.

1.1.4 Classification

The images are categorized according to the extracted features from the images. Classification usually plays an important role to determine the performance of an algorithm. Classification can be successful even for low-resolution images and it is important to recognize images. There are many classification methods that are successfully classifying human beings according to their biometric characteristics.

The rest of the thesis is as follows. In Chapter 2 of this thesis, previous work done and related work will be reviewed about palmprint recognition for the past years, and what researchers have done to improve those algorithms. In Chapter 3, the feature extraction methods will be investigated such as Principal Component Analysis, Discrete Cosine Transform, Local Binary Patterns, Log-Gabor and for each method the properties will be explained. In Chapter 4, the results of the experiments will be shown according to each algorithm and the advantages and disadvantages of each algorithm will be shown. Finally, in the last chapter, the conclusion will be given about the experimental results obtained for each algorithm.

Chapter 2

PREVIOUS WORK ON PALMPRINT RECOGNITION

2.1 Historical Review About Biometric Recognition

Biometrics technology is an important application in image processing area and it is becoming more and more popular day by day. Nowadays, in most of the countries, the researchers concentrate and try to improve this field because biometrics play a significant role in security field. It was useful to analyze many security cases and that became a strong reason to push researchers to do more researches and more developments in this field. Moreover, biometrics technology plays an important role not only in the security field, but also in commercial, civil and industrial projects by including recognition and identification of human beings within these projects. A detailed history about biometrics technology is given below.

2.2 Biometrics History

Biometrics is a word that contains two merged words in Greek language. The first part “bio” comes from the term life, and the second part “metrics” means measurement. Therefore, the term biometrics means life measurement [7].

The biometric systems have appeared in the twenty first century and it became an interesting topic for all researchers after realizing the effects of biometrics in image processing. All the attention in that century was to use biometrics in recognition and identification area using palmprint, iris, fingerprint, face and other physical or behavioral biometrics.

The history of biometrics is very old. Many years ago, it has been used by Chinese and Egyptian people in different ways [8] [9] [7]. In this chapter, a very brief history of biometrics systems will be given and related work for palmprint recognition will be discussed in detail.

In 1858, Sir W. Herschel, in Civil Service of India was the first in the world who took palm and hand images and put them at the end of the contracts for identification issues [9] [7]. Few years later in 1870, a new method developed for identification, in which the name of the system was Bertillonage. The method worked according to the human body's measurements [9] [7].Later on in 1892, Henry classification technique for finger and palmprint recognition has been developed by Sir E. Henry. Since then, the system has been used. Four years later, in 1896, F. Galton developed a way to identify thousands of palmprint images to recognize criminals. Then in 1901, Sir E. Henry. invented the first fingerprint classification method which became the first official system in England at that time [9] [7].

A few years later, in 1903, US jails were first to apply fingerprint and palmprint identification systems. Furthermore, in 1905, it had been applied in military bases in US. A few years, it had been applied in police stations. Three years later, in 1908, fingerprint card for the first time had been invented. Moreover, in 1917, palmprint identification system had been developed in Nevada [9] [7].

In 1974, for the first time, a commercial hand system became available for access control for taking attendance and performing personal identification. This system had been used in many big organizations such as FBI and NIST. A few years later, in 1980, for the first time they had created a big database for fingerprints for an Identification System (AFIS) in United States. This system is working even now with around 70 million cards or nearly 700 million individuals [9] [7].

In 1994, Automated Fingerprint Identification System had been designed for palmprint and fingerprint identification by a Hungarian company, and this system had been sold in the year 1997 to the US companies [9] [7]. Then, in 1996, a hand geometry system had been designed to manage and protect Olympic Village in US. This system was applied on 65,000 population of the village for duration of 28 days. They have more than one million operation access on this system. Researchers are still working on designing powerful palmprint recognition systems by using many different techniques.

2.3 A Survey on Palmprint Recognition Methods

In most of the studies, palmprint recognition had been applied on small databases. A detailed information about palmprint recognition studies using Log-Gabor, LBP, DCT and PCA methods is given below.

In 2002, W. Kong and D. Zhang had used 2D Gabor filter for palmprint recognition with hamming distance classification. The evaluation had been done based on a database with 435 low resolution samples for 95 individuals. Their results show that FAR (False Acceptance Rate) was 0% when threshold value was fixed at 0.335 and FRR (False Rejection Rate) was 0.9% for image resolution of only 65 dpi. [10].

One year later in 2003, D. Zhang et al. had applied 2D Gabor filter on low resolution templates and for classification they used Hamming distance. Their results shows that EER (Equal Error Rate) was 0.6%, the calculated total time for identification was 1.1 second with a database that contains images for 7752 individuals for 386 individuals. Their performance as Genuine Acceptance Rate (GAR) was 98% and FAR was 0.4% with EER 0.6% [6].

Later on in 2004, L. Zhang and D. Zhang proposed another approach for palmprint recognition by extracting features with Wavelet transform. Their performance shows that the new approach can identify the people at 98% correctly. This simulation had been done based on a database that contains 150 low-resolution samples for 50 individuals [11]. Again in 2004, X. Jing and D. Zhang had applied discrete cosine transform (DCT) on the face and palmprint recognition for the first time. The system was using two-dimensions of separability judgment to select the frequency bands with favorable linear separability depending on the selected bands, the features were extracted and they obtained 97.5% recognition accuracy [12].

In 2005, J. Noh and K. Rhee proposed a new palmprint recognition method. They had depended on Hu invariant moment and it had been applied on a small low-resolution database. Their performance showed that the recognition rate with their database reaches up to 98.1% [13].

In the year of 2005, A. Kumar and D. Zhang had divided the information of palmprint into three types namely texture based such as (Gabor) and wavelets, line based such as

DCT, appearance based such as Eigenpalm and Fisherpalm. The three types of information had been combined using Gabor, DCT and PCA approaches. They did a simulation with 100 users and their performance shows that they enhanced the performance by 34.56% in EER by the developed method [14] [15].

In the year of 2008, M. Ekinci and M. Aykut had introduced another method, which was working by combining PCA method by Gabor wavelet for palmprint recognition. They applied the method on PolyU-II database, which has 7752 images for 386 individuals. Their results showed that it has an accuracy of 94.571% [16].

In 2011, Meiru Mu et al. had developed a new method to extract features for palmprint identification. Their method was taking the advantage of combining two different algorithms. The shiftable complex directional filter bank (CDFB) transform and the local binary patterns (LBP) have been combined. The results showed that CDFB performs better results in terms of identification accuracy, storage requirements and computational complexity. Moreover, the lower redundancy information of CDFB transform generates less LBP histogram bins which make it to achieve higher identification accuracy [17].

In 2014, Linlin Shen et al. had designed a 3 dimensional Gabor filter. Their simulation were based on orientation and frequencies which can be obtained with Gabor wavelets. A cube shape was given to the extracted features for getting transformed to joint spatial domain and the maximum value for the wavelets of each 3D cube were considered as a phase and were coded with two bits and used for classification. Moreover, they had applied the proposed method on PolyU database which has 380 samples and the performance was 4% equal error rate (EER) [18].

Chapter 3

FEATURE EXTRACTION METHODS

In pattern recognition, the most important characteristic is feature extraction. Feature extraction is the process to extract the most important features which are useful for classification. Generally, feature extraction algorithms can be performed in two main categories namely feature extraction process which can be applied in spatial domain and feature extraction process which can be applied in frequency domain. The algorithms which require to be applied in frequency domain have to be transformed from spatial domain into frequency domain in order to extract features.

The feature extraction algorithms which has been used in this thesis, are described below. These are namely Principal Component Analysis, Discrete Cosine Transform, Local Binary Patterns and Log-Gabor filters.

3.1 Principal Component Analysis (PCA)

Principal Component Analysis is a statistical approach invented by Karl Pearson to predict the classes for high dimensional data in 1901 [19]. It is useful for describing a large dimensional space with a relative small set of vectors. It has a significant role in finding patterns of high dimensional data [20]. It is called Eigenpalm whenever PCA is applied on palmprint images.

PCA can be described as a transformation function as well. It converts the data from high dimension into lower dimension. The main idea of this approach is to compress the data by lossy compression technique [21]. The approach works by minimizing the number of dimensions of the data. The steps to extract features by using PCA are described below:

Step1: Read images

Suppose that all the images in the dataset are arranged as a set of n data vectors $x_1, x_2, \ldots, x_n$ with each x_i defining a single grouped observation of the p variables. Take $x_1, x_2, \ldots, x_n$ as row vectors, each of which has p columns. The resulting n*x*p dimension matrix is referred to as X.

Step2: Calculate the mean of images

Calculate the mean m along each dimension j= 1,…,p which is the sum of all the training images divided by the total number of training images N. The calculated mean values are represented into a vector m of size p*x*1 as

$$m[j] = \left(\sum_{i=1}^{n} X[i,j]\right) * 1/N \qquad \textbf{(3.1)}$$

Step3: Mean subtraction

Mean subtraction is required to make sure that the initial principal component defines the direction of maximum variance. Subtract the vector m from each row of the data matrix X and save the result in the n *x* p matrix B as

$$B = X - hm^T \qquad \textbf{(3.2)}$$

where h is an n*x*1 column vector consisting of ones.

$$h[i] = 1 \text{ for } \; i = 1, \ldots, n \qquad \textbf{(3.3)}$$

Step4: Calculate the covariance matrix

Calculate the p*x*p covariance matrix C using the following formula:

$$C = \frac{1}{n-1}\ B.B^T \qquad \textbf{(3.4)}$$

where B^T is the transpose of matrix B.

Step 5: Calculate the eigenvectors and eigenvalues of the covariance matrix

The matrix V of eigenvectors contains useful information about our data which diagonalizes the covariance matrix C. As the covariance matrix C is square, we can easily find the eigenvectors and eigenvalues for this matrix.

$$\mathrm{D} = \mathrm{V}^{-1}\mathrm{CV} \qquad \textbf{(3.5)}$$

The matrix *D* is M*x*M diagonal matrix of eigenvalues of C. Matrix *V* is p*x*p dimension and consists of p column vectors. Each column vector has p length, which shows the p eigenvectors of the covariance matrix C.

Step 6: Sort the eigenvectors and eigenvalues

While maintaining the correct pairings between the columns in each matrix, sort the columns of the eigenvector matrix V by eigenvalue matrix D, from the highest to the lowest. This gives you the components in order of significance.

Step 7: Choose components and form the basis vectors

The eigenvector with the highest eigenvalue is the principal component of the data set. At this time, it is possible to ignore the components of lesser importance. This causes loss of some information, but if the eigenvalues are small, the loss is insignificant. Leaving some components out, causes the final data set to have less dimensions than the original.

A basis vector is constructed by taking the first L eigenvectors of V that are chosen from the list of eigenvectors, and forming a p*x*L matrix W with these eigenvectors in the columns.

$\mathrm{W}[\mathrm{k},\mathrm{l}] = \mathrm{V}[\mathrm{k},\mathrm{l}]$ for $\mathrm{k} = 1, \ldots, \mathrm{p}$ and $\mathrm{l} = 1, \ldots, \mathrm{L}$, where $1 \leq L \leq p$. **(3.6)**

Step 8: Projection

By considering the similarity degree, the projection matrix of every training image is compared with the test image's projection matrix. The output will be the image with the maximum similarity to the test image.

3.2 Discrete Cosine Transform (DCT)

Discrete Cosine Transform is one of the transformation approaches for palmprint recognition and it has been invented by Ahmed, Natarajan and Rao for the first time [22]. It has eight different versions and each version has two types which are even or odd type. The versions which can be used in image processing field are DCT-I, DCT-II, DCT-III and DCT-IV with the even type. DCT-II is represented in Equation 3.8 as below:

$$[C_N^{II}] = \sqrt{\frac{2}{N}} \left[\varepsilon_K \cos\frac{\pi(2_n + 1)K}{2N}\right] \quad n, k = 0,1, \ldots., N-1 \tag{3.7}$$

$$\varepsilon_K = \begin{cases} \frac{1}{\sqrt{2}}, & p = 0 \; or \; p = N \\ 1 \;, & otherwise \end{cases} \tag{3.8}$$

In image processing and recognition, DCT plays a significant role to reduce information redundancy in the images. The reason is that it transforms necessary coefficients and the information that can be obtained from compression and decompression operations or features that are related to transform coding systems. For applying this transformation, a function named sinusoidal basis must be applied. The sinusoidal basis function takes the advantage of using only cosine functions and eliminating the sine functions. Discrete Cosine Transform operations are explained below in detail.

3.2.1 The Discrete Cosine Transform Operations

The first step is directing DCT transformation to the signal in order to move the signal from spatial domain into frequency domain. This process makes the DCT coefficients to be appeared in frequency domain. The coefficients can be categorized into three parts in frequency domain. The first part is related to the coefficients which are located in the lowest part of the frequency. This part holds the most representative information from the original signal. The second contains the last coefficient with more detailed signal. It is located in the higher frequencies and the detail of the signal is the effect of noise which is caused by transformation [23]. The third part is the part, which is located between the lowest and the highest part, and the last coefficients in this part hold different information of the original signal.

DCT is playing a significant role to reduce image information redundancy in the field of image processing, because it takes some necessary transform coefficients to present the important features which are necessary [24]. For palmprint recognition with DCT, the classification starts by extracting DCT coefficients and then continues by measuring the distance between DCT coefficients for train and test palm images. The minimum distance between DCT cosecants is the most resembling palm to the same person.

3.2.2 One-dimensional DCT

The suitable directions for multidimensional transforms can be disintegrated in one-dimensional (1-D) transforms. The first step to extract coefficients from the image is transforming the image from spatial domain waveform into frequency domain based on one dimension of DCT (DCT-II). The set of coefficients will represent DCT transformation and this process for one dimensional DCT is represented in Figure 3.1

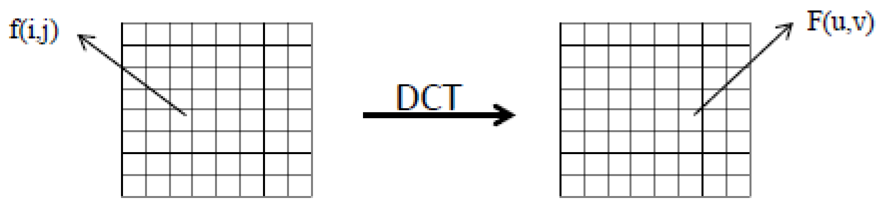

Figure 3.1: One-dimensional DCT process [24]

The formula for one-dimensional DCT is as follows:

$$F(u) = a(u) \sum_{X=0}^{N-1} f(x).\cos\left[\frac{\pi(2x+1)u}{2N}\right] \qquad \textbf{(3.9)}$$

where $a(0) = \sqrt{\frac{1}{N}}$, $a(m) = \sqrt{\frac{2}{N}}$ with $m > 0$,

u represents the input row of the image, *N* is the total number of coefficients and *x* is the first coefficient in a row.

The function of the IDCT can be demonstrated as

$$\mathrm{f(u)} = \sum_{\mathrm{x}=0}^{\mathrm{N}-1} \mathrm{a(u)f(x)}.\cos\left[\frac{\pi(2\mathrm{x}+1)\mathrm{u}}{2\mathrm{N}}\right] \qquad \textbf{(3.10)}$$

where $a(0) = \sqrt{\frac{1}{N}}$, $a(m) = \sqrt{\frac{2}{N}}$ with $m > 0$,

u represents the input row of the image, *N* is the total number of coefficients and *x* is the first coefficient in a row.

3.2.3 Two-dimensional DCT

The generation of two dimensional (2-D) DCT is done by applying two times 1-D DCT to an image, once by rows and then by columns [25] [26]. The DCT definition of an image can be computed as follows:

$$F(u,v) = \frac{2}{\sqrt{MN}} a(u)a(v) \sum_{x=0}^{N-1} \sum_{y=0}^{M-1} f(x,y) \cos\left[\frac{(2x+1)u\pi}{2N}\right] \cos\left[\frac{(2y+1)v\pi}{2M}\right] \tag{3.11}$$

$$F(u,v) = \frac{2}{\sqrt{MN}} \sum_{u=0}^{N-1} \sum_{V=0}^{M-1} a(u)a(v)C(u,v) \cos\left[\frac{(2x+1)u\pi}{2N}\right] \cos\left[\frac{(2y+1)v\pi}{2M}\right] \tag{3.12}$$

where u represents the input row of the image and v represents the input columns. N is the total number of coefficients in a row and M is the total number of coefficients in a column. x is the first coefficients in a row and y is the first coefficients in a column. The process of two dimensional DCT can be applied as shown in Figure 3.2.

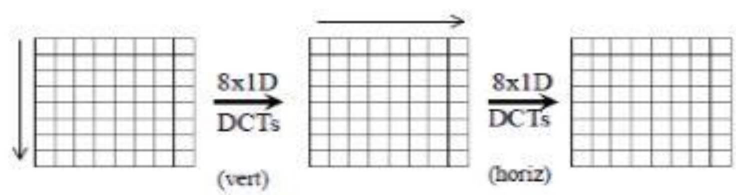

Figure 3.2: Two-dimensional DCT operation [24]

3.2.4 Reorganization Process for DCT Coefficients

The first stage in the recognition of the DCT coefficients starts by dividing the image into subregions. The next stage is to apply transformation function on each subregion. Moreover, each subregion will be transferred into DCT domain individually. Then, the values for DCT coefficients will be categorized into two parts the first part is with small and useless values in which DCT coefficients mostly exist in it. This information will be removed if the value of coefficients is less than threshold amount. The other part contains the large and useful values. For some images, the large values are located in the upper-left corner of DCT [24] [27].

3.2.5 Classification of DCT Coefficients

After extracting DCT coefficients and useful information of each palm image, the classification starts by measuring the distance between DCT coefficients of train and test palm images. The minimum distance between DCT cosecants is the most resembling palm to the same person.

There are many algorithms for classification, each of them having their own advantage and disadvantage. In this thesis, k-nearest neighbor (KNN) has been used to classify the test images.

3.3 Log-Gabor Filters

Log-Gabor is an advanced filter of Gabor filters. Therefore, a brief explanation about Gabor filters will be given before the description of Log-Gabor filters.

Dennis Gabor invented Gabor filters in 1946. The filter gives the best representation for signals in spatial and frequency domain, where the signals are in the best conjoint representation.

Gabor filters can be implemented by combining Gaussian with sine and cosine waves. This process produces a unique conjoint localization in both frequency and spatial domains. These localizations are in a way that sine and cosine waves in the frequency domain are localized in a very good way, while in the spatial domain, it doesn’t provide a good localization. At the same time, Gaussian is giving a very good localization in the spatial domain space. The combination process makes Gabor to give a good localization in both frequency and spatial domain by taking the advantage of sine and cosine waves and Gaussian function.

The decompression process after applying Gabor is producing two parts (imaginary and real). By applying Gaussian, the real part is produced and sine/cosine waves are producing the imaginary part. Figure 3.3 shows real and imaginary parts of a Gabor filter. Another name given to real and imaginary part is even symmetric and odd symmetric. The bandwidth and center of the frequency are getting specified for the filter. Gaussian width is specifying the bandwidth and, sine and cosine waves are specifying the center of frequency. The formula below represents Gabor filter with two dimension (*x*,*y*) specified for an image.

$$G(x,y) = e^{-\Pi[(x-x_0)^2/a^2 + (y-y_0)^2/\beta^2]} e^{-2\Pi[u_0(x-x_0)+v_0(y-y_0)]} \quad \textbf{(3.13)}$$

As it is shown in the above formula, (x_0, y_0) are representing the position of the pixels and (α,β) is representing the width and length of the Gaussain, and (μ_0, v_0) represents the modulation with the spatial frequency $\omega 0 = \sqrt{\mu_0^2 + v_0^2}$.

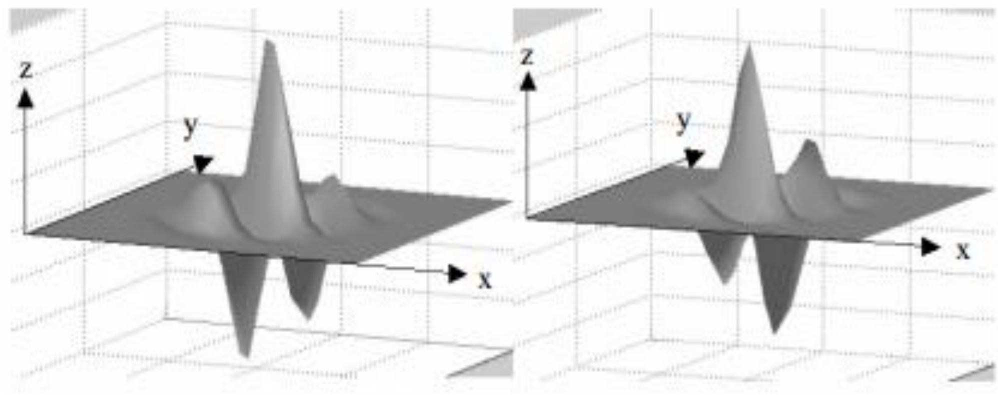

Figure 3.3: The Imaginary and Real Part in Gabor [28]

Log-Gabor is an advanced filter of Gabor filter. It is an edge detector that gives a strong response for locations of images. This localization is made by applying the Gabor Transform. The Gabor filter is basically a Gaussian function. One of the disadvantages of Gabor is that it is an even symmetric filter that produces DC component when the bandwidth is bigger than one octave. In order to enhance the filter, logarithmic scale has been used for Gaussian. By taking the logarithmic version, it produces zero DC for any bandwidth.

The Gaussian value of the image can be used to extract palmprint features by applying the following formula:

$$G(f) = \exp\left[\frac{-\left(\log\left(\frac{f}{f_0}\right)\right)^2}{2\left(\log\left(\frac{\sigma}{f_0}\right)\right)^2}\right] \tag{3.14}$$

where fo represents the center frequency, and σ gives the bandwidth of the filter. In the experiments, the parameters of Log-Gabor filter were empirically selected as fo =1/2 and σ was assigned different parameter values.

The result of 1D Log-Gabor filter must be utilized as a basic feature. By applying the filter, the features are generated from the ROI. The results obtained using real and imaginary parts are combined in the log-Gabor phase response, Ψ, as follows:

$$\Psi = \tan^{-1}\left(\frac{\Phi_i}{\Phi_r}\right) \quad \textbf{(3.15)}$$

The outcome of log-Gabor is encoded by Ψ that is qualitatively encoded as '1' or '0' based on the sign to obtain the template ϕ. Therefore, each point in the Ψ is coded to one bit by the following inequalities:

$$\varphi(i,j) = \begin{cases} 1 & if\ \ \Psi(i,j) \geq 0 \\ 0 & if\ \ \Psi(i,j) < 0 \end{cases} \quad \textbf{(3.16)}$$

The matching between an input and a stored template consists of computing matching scores (degrees of similarity or dissimilarity) between them. The matching task in experimental schemes is based on a normalized Manhattan distance. It is defined as the number of places where two vectors differ.

Figure 3.4 shows Log-Gabor feature extraction process. In the first steps, 1D Log-Gabor filter is applied on palm images [28]. Then, outputs of the filter which are even symmetric and odd symmetric parts are getting combined and phase quantization is created based on these combinations. In order to prepare the phase quantization for matching, the phase quantization are coded by (0,1) bits to obtain a template for matching.

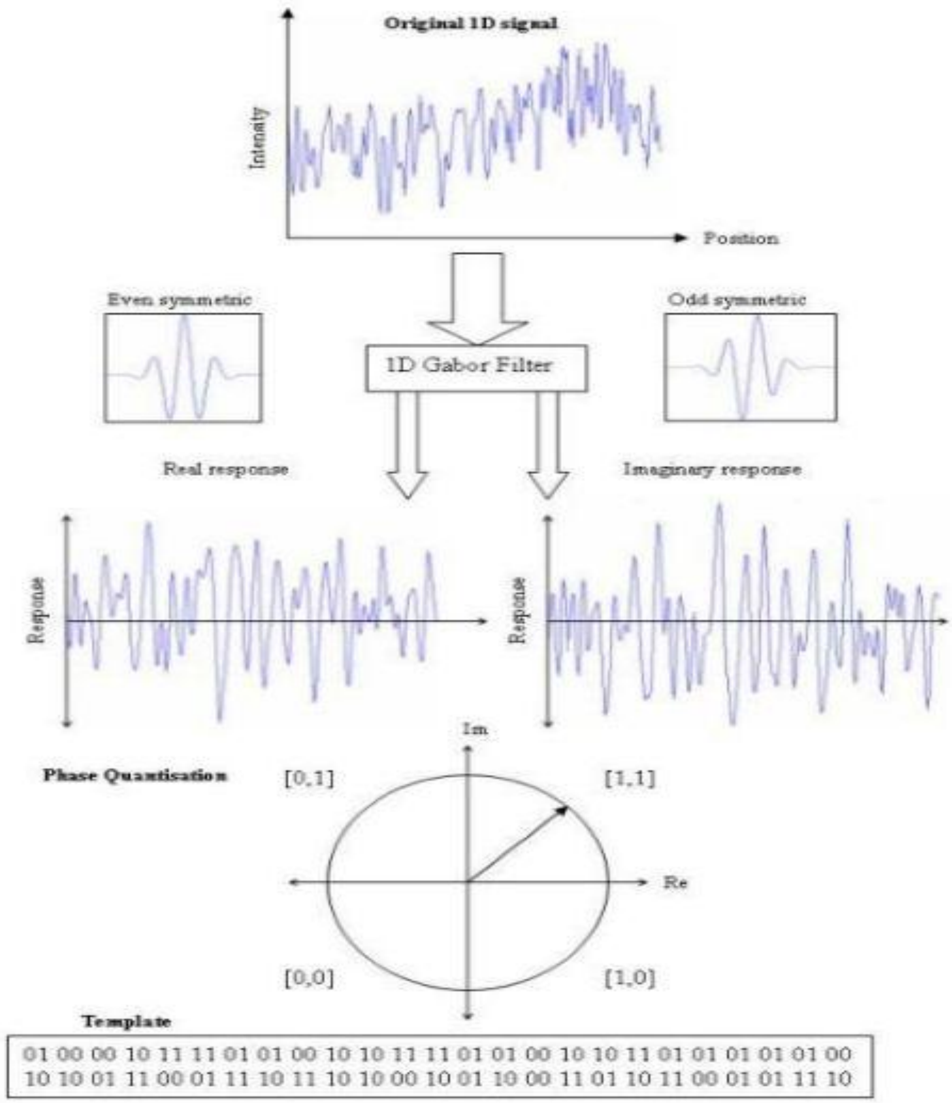

Figure 3.4: Log-Gabor Feature Extraction Process [28]

3.4 Local Binary Patterns (LBP)

In 2006, Ahonen et al. had invented LBP based face description. The method works by creating some blocks inside the image, then inside each block, LBP textures are getting extracted. These extractions are based on converting the texture lines inside each block into feature histograms. Then, these feature histograms are concatenated to make local descriptions. LBP is applied for each pixel and it creates a binary number for each block.

In the next step, by benefitting of the binary code, the texture features can be created for each block. In the final step, it combines all the histograms of the texture features to create the code for the image.

In order to get benefit from different scales of the textures in LBP operations, researchers expanded the neighborhood usage by using different sizes inside LBP operations as shown in Figure 3.5

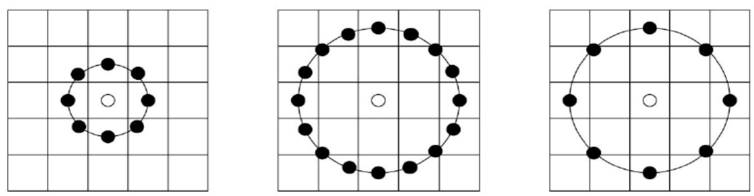

a) p = 8, r = 1 b) p = 16, r = 2 c) p = 8, r = 2

Figure 3.5: Circular neighborhood in LBP [29]

The first step in LBP implementation is to select the number of regions. In case the number of selected regions is assumed as 5*5, then the size of the image must be divisible by 5. If the image size is not divisible by 5 then the image must be resized to an approximate size. For example, an image with the size of (64rows*80columns) cannot be divided into 5*5 regions. It is not possible to do it directly because the size of the local regions will not be an integer number. In this case, the image must be resized into (60*80) and the block size will be (12*16).

The second step of LBP implementation is the blocking process. In this stage, each local region is considered to be a block and the LBP operations are applied on each block separately. In this stage, the center pixel of the block will be selected, and the neighbor values around the centered pixel will be compared to the pixels which are neighbors of the centered pixel. In case the value of the center was bigger than the neighbors, the label is getting 0, otherwise it gets 1 as a label. As it is shown in Equation 3.21, the values of the center and the neighbors are compared to create label value for each region or block.

$$LBP_{(p,r)}(X_C) = \sum_{P}^{P-1} u\left(X_p - X_C\right)2p \tag{3.17}$$

$$u_y = \begin{cases} 1, & y \geq 0 \\ 0, & y < 0 \end{cases} \tag{3.18}$$

As it is shown in the above equations, the (x_c) is the value of the centered pixel, and (x_p) is the value of the sample pixel, and (p,r) is representing the neighborhoods pixel , where p is the sampling number of points on a circle of radius r. An example of LBP computation is shown in Figure 3.6 and an LBP mathematical operation is shown in Figure 3.7.

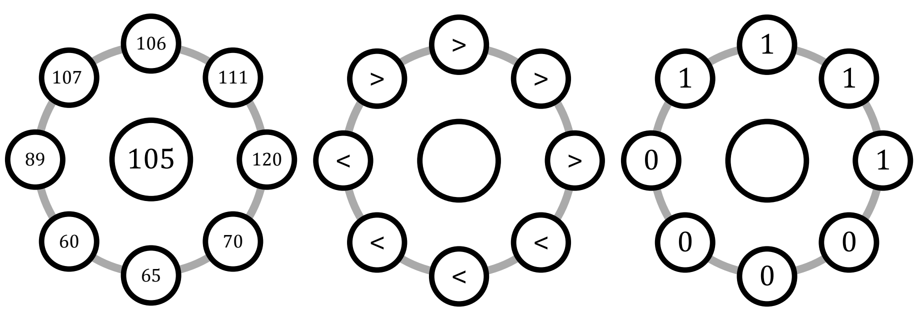

Figure 3.6: LBP Computation Sample [29]

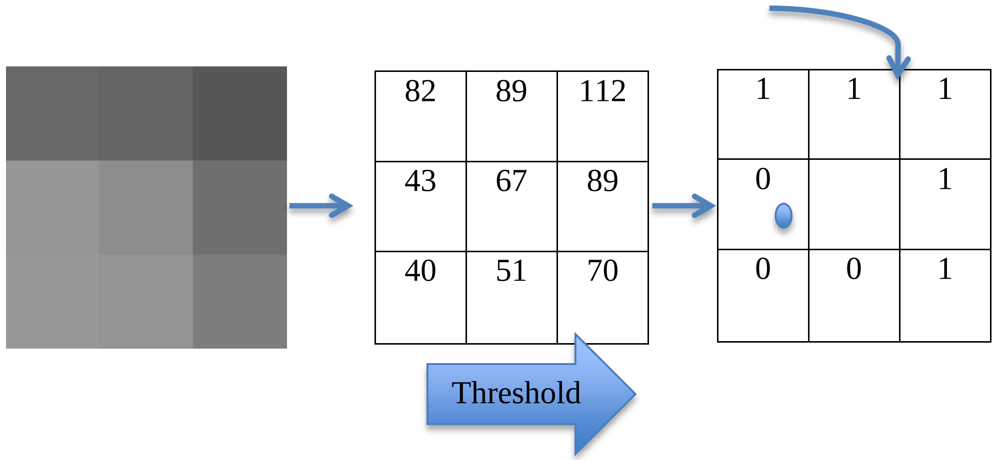

Figure 3.7: LBP Mathematical Operation [29]

Chapter 4

EXPERIMENTS AND RESULTS

Performance evaluation of the best feature extraction algorithm for palmprint recognition has been studied on PolyU database. In this thesis, we have investigated different scenarios and different situations to evaluate each algorithm. The four algorithms namely PCA, DCT, LBP and Log-Gabor have been compared by using MATLAB programming platform.

4.1 Palmprint Database

PolyU is a public touchless palmprint image database. It consists of the hand images collected from the students and staff of Polytechnic University at IIT Delhi, India. The database has been acquired in the Biometrics Research Laboratory by using a digital CMOS camera. The acquired images were saved in bitmap format.

The aim of creating this database is to make a standard database to help researchers to do more studies about biometric recognition. The database has been used for many studies and it became a standard palmprint database for the researchers.

The database has been created during July 2006 - Jun 2007. Moreover, the database contains left and right hand images from 235 subjects. The total number of images in the database for the right and left hand are 2601 images, 1301 images belong to the left hand and 1300 images belong to the right hand. All the subjects in the database are in the age group of 14-56 years with resolution of 800*600 before cropping and selecting region of interest (ROI). After extracting ROI, the resolution of images became (150*150) and each class has 5 to 7 hand image samples from each of the hands.

4.2 Experimental Results

The experimental results are categorized into four sections. The results obtained from each algorithm namely PCA, DCT, LBP and Log-Gabor are demonstrated in the following subsections.

4.2.1 Performance Evaluation Using PCA

Performance evaluation has been done on various experimental setups. The number of train and test images are increased in each experiment set from 150 to 470 images for both left and right palmprint datasets. The results are demonstrated on Figure 4.1. For the right and left palmprint datasets, the tables below represent the evaluation performance for PCA. Four images have been selected for each class, two of them were used as train images and the remaining two images were used for testing. Table 4.1 represents the performance evaluation for right hand and Table 4.2 represents performance evaluation for left hand. On the other hand, different number of eigenvectors are selected in the test set of experiments on PCA. Table 4.3 represents the evaluation performance for PCA with different number of eigenvectors used in the algorithm.

Table 4.1: PCA Performance Evaluation on Right Palmprint Dataset

Experiment Set	Number of Train Images	Number of Test Images	Recognition Rate (%)
1	150	150	76.67
2	200	200	74.50
3	250	250	70.00
4	300	300	73.34
5	350	350	74.29
6	400	400	74.50
7	450	450	73.78
8	470	470	74.90

Table 4.2: PCA Performance Evaluation on Left Palmprint Dataset

Experiment Set	Number of Train Images	Number of Test Images	Recognition Rate (%)
1	150	150	75.34
2	200	200	75.50
3	250	250	74.00
4	300	300	72.67
5	350	350	71.72
6	400	400	71.76
7	450	450	74.23
8	470	470	74.69

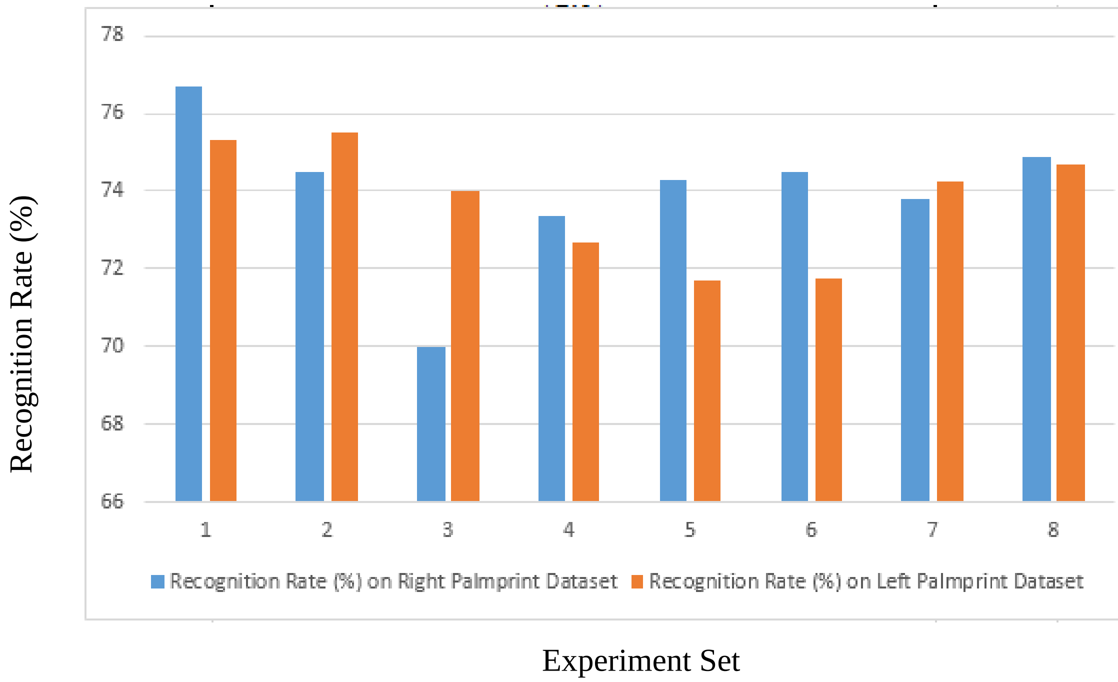

Figure 4.1: Performance Evaluation (%) using PCA

Table 4.3: PCA Performance with Different Number of Eigenvectors for Left and Right Palmprint Datasets.

Number of Eigenvectors	**Recognition Rate (%) Left Palmprint Dataset**	**Recognition Rate (%) Right Palmprint Dataset**
100	64.90	66.81
150	67.00	68.32
200	69.79	70.23
250	73.40	71.68
300	75.32	72.56
350	75.32	74.00
400	75.32	74.90
450	74.50	74.90
469	74.69	74.90

4.2.2 Performance Evaluation Using LBP

The performance evaluation for LBP has been investigated by doing different experiments. The tables bellow shows different experiments for LBP by selecting two types of neighborhoods as (1,8) and (2,8) for the right and left hand by applying on 235 individuals. Four images have been selected for each individual, two as train images and two as test images. Table 4.4 shows performance evaluation for right and left hand with neighborhood of (1,8) and (2,8). The experiments are performed with a number of pattern size starting from 5*5 partitions up to 13*13 partitions on the cropped palmprint images of size 150*150. The results are also demonstrated on Figure 4.2 and Figure 4.3 for left and right palmprint datasets, respectively.

Table 4.4: LBP Performance Evaluation for Left and Right Palmprint Datasets

Pattern Size	**Recognition Rate (%)**			
	Right		**Left**	
	(1,8)	(2,8)	(1,8)	(2,8)
5X5	81.7021	57.2340	84.0426	61.9149
6X6	87.8723	71.9149	86.5957	75.1064
7X7	90.0000	84.8936	89.1489	85.7447
8X8	92.1277	90.0000	92.1277	88.5106
9X9	90.6383	92.1277	92.1277	91.7021
10X10	93.4043	94.0426	91.4894	92.9787
11X11	91.0638	94.0426	92.3404	93.6170
12X12	93.1915	94.6809	92.5532	95.7447
13X13	90.2128	94.2553	89.5745	94.0426

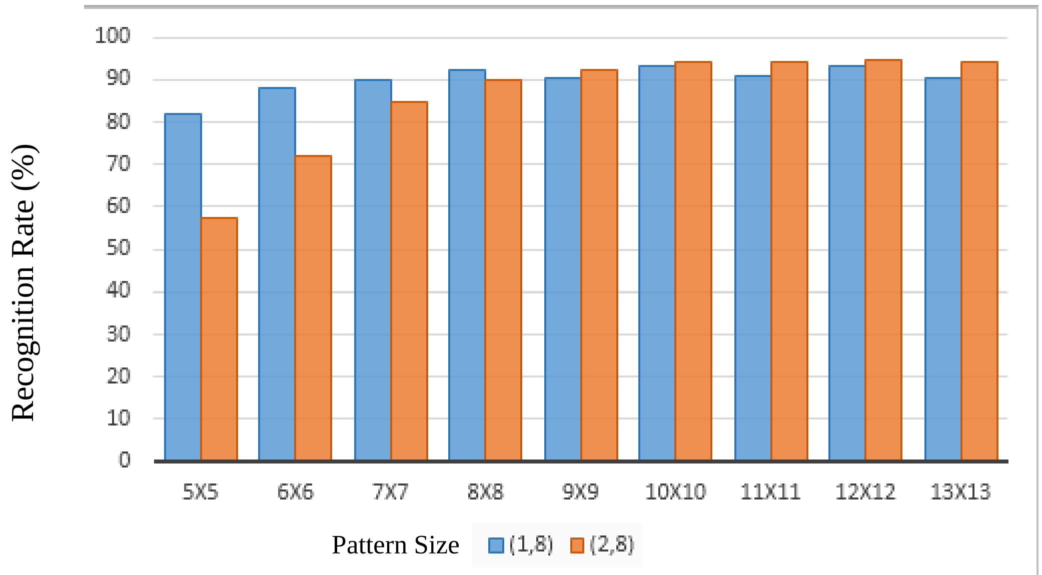

Figure 4.2: Performance Evaluation on Right Palmprint Dataset using LBP

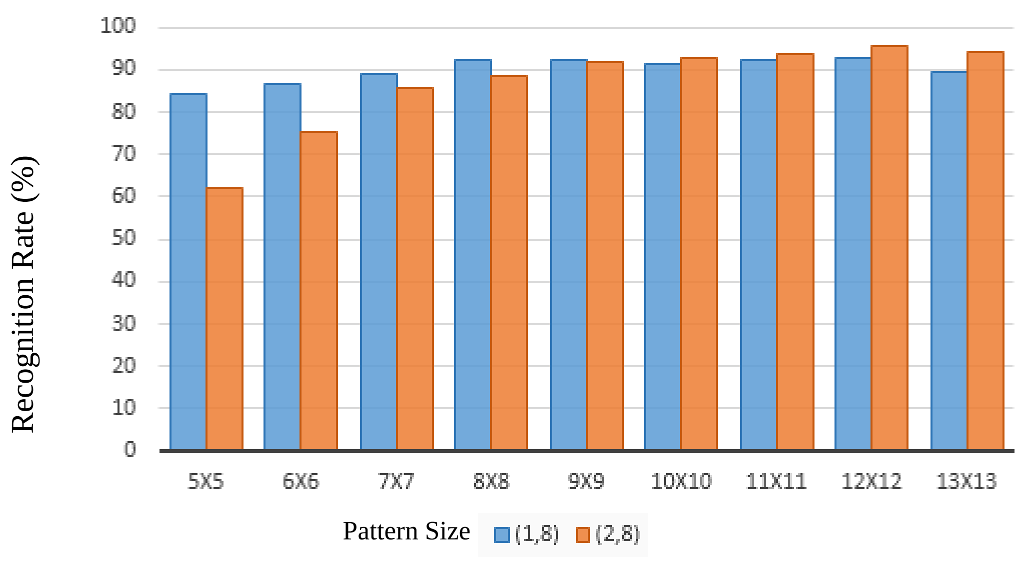

Figure 4.3: Performance Evaluation on Left Palmprint Dataset using LBP

4.2.3 Performance Evaluation Using DCT

The performance evaluation for DCT has been investigated by doing different set of experiments. The tables show various experiments applied on different number of users. The experiments are carried out by using 4 images for each class; two images are used as train and the remaining two images are used as test images. Table 4.5 and 4.6 present the performance evaluation for right and left palmprint datasets using DCT.

Table 4.5: DCT Performance Evaluation on Left Palmprint Dataset

Experiment Set	Number of Train Images	Number of Test Images	Recognition Rate (%)
1	150	150	83.3333
2	200	200	83.5
3	250	250	86
4	300	300	85.6667
5	350	350	85.7143
6	400	400	86
7	450	450	84.4444
8	470	470	84.0426

Table 4.6: DCT Performance Evaluation on Right Palmprint Dataset

Experiment Set	Number of Train Images	Number of Test Images	Recognition Rate (%)
1	150	150	80.6667
2	200	200	80
3	250	250	78
4	300	300	78.3333
5	350	350	79.1429
6	400	400	79.7500
7	450	450	79.7500
8	470	470	80.4255

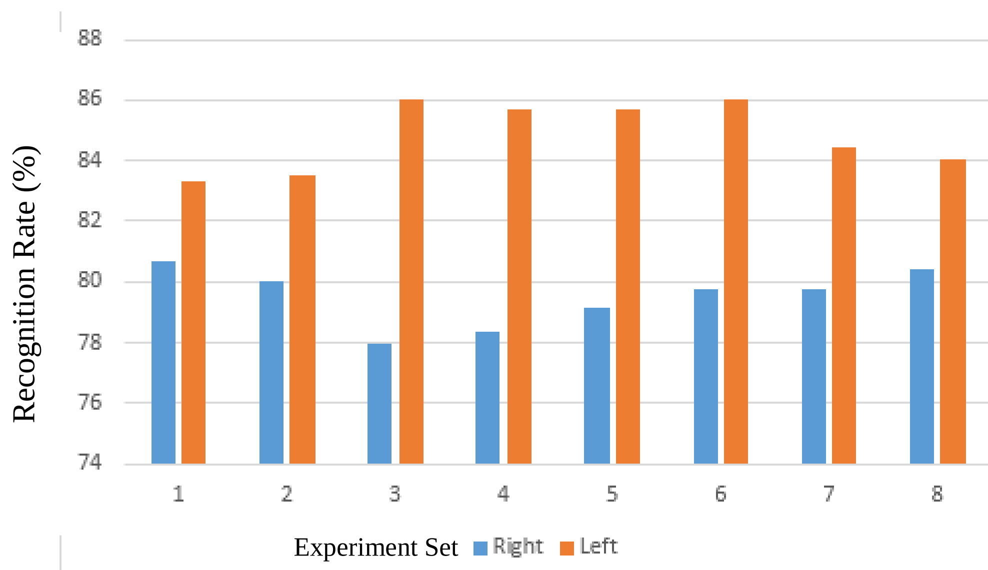

Figure 4.4: Performance Evaluation using DCT

4.2.4 Performance Evaluation Using Log-Gabor

The experiments performed using Log-Gabor approach have been performed by employing 235 classes on both left and right palmprint datasets. Four images were used in these experiments for each class where two images are used for training and the remaining two for testing for right and left hand. As it is shown in the tables below, the performance is changing by modifying the values of parameters of the filter. Each table represents the performance for a specific sigma value with different values for wavelength. The following tables represent performance evaluation using both left and right palmprint datasets with different wavelength ranges changing from 10 to 60. Tables 4.7 to 4.10 demonstrate palmprint recognition rates using sigma values of 0.45, 0.55, 0.6, 0.65, respectively. These results are summarized in Figure 4.5 on left palmprint dataset with each sigma value using Log-Gabor with the best wavelength value. On the other hand, Tables 4.11 to 4.14 demonstrate palmprint recognition rates on right palmprint dataset using the same set of sigma values as mentioned above. The results for these experiments are summarized in Figure 4.6 for each sigma value with the best wavelength.

Table 4.7: Log-Gabor Performance Evaluation for Left Hand by Using Sigma (0.45)

Experiment	**Wavelength**	**Recognition Rate (%)**
1	10	68.0851
2	11	69.5745
3	12	70.4255
4	13	71.0638
5	14	71.4894
6	15	72.5532
7	16	73.6170
8	17	75.3191
9	25	80
10	30	81.2766
11	35	81.2766
12	40	81.4894
13	45	80.6383

Table 4.8: Log-Gabor Performance Evaluation for Left Hand by Using Sigma (0.55)

Experiment	**Wavelength**	**Recognition Rate (%)**
1	10	64.0426
2	11	65.5319
3	12	67.2340
4	13	68.2979
5	14	69.5745
6	15	70.6383
7	16	71.2766
8	17	71.7021
9	20	74.8936
10	25	78.0851
11	30	80.6383
12	35	80.6383
13	40	80.4255
14	45	80.4255
15	50	80.8511
16	60	79.1489

Table 4.9: Log-Gabor Performance Evaluation for Left Hand by Using Sigma (0.6)

Experiment	**Wavelength**	**Recognition Rate (%)**
1	10	62.3404
2	11	63.8298
3	12	65.5319
4	13	66.1702
5	14	67.2340
6	15	68.5106
7	16	69.5745
8	17	70.8511
9	18	72.1277
10	20	73.8298
11	25	76.5957
12	30	79.5745
13	35	80.2128
14	40	79.7872
15	45	79.5745

Table 4.10: Log-Gabor Performance Evaluation for Left Hand by Using Sigma (0.65)

Experiment	Wavelength	Recognition Rate (%)
1	10	58.2979
2	11	61.9149
3	12	62.7660
4	13	64.4681
5	14	66.5957
6	15	67.0213
7	16	68.0851
8	17	69.7872
9	20	71.9149
10	25	74.2553
11	30	77.2340
12	35	78.9362
13	40	79.3617
14	45	78.7234

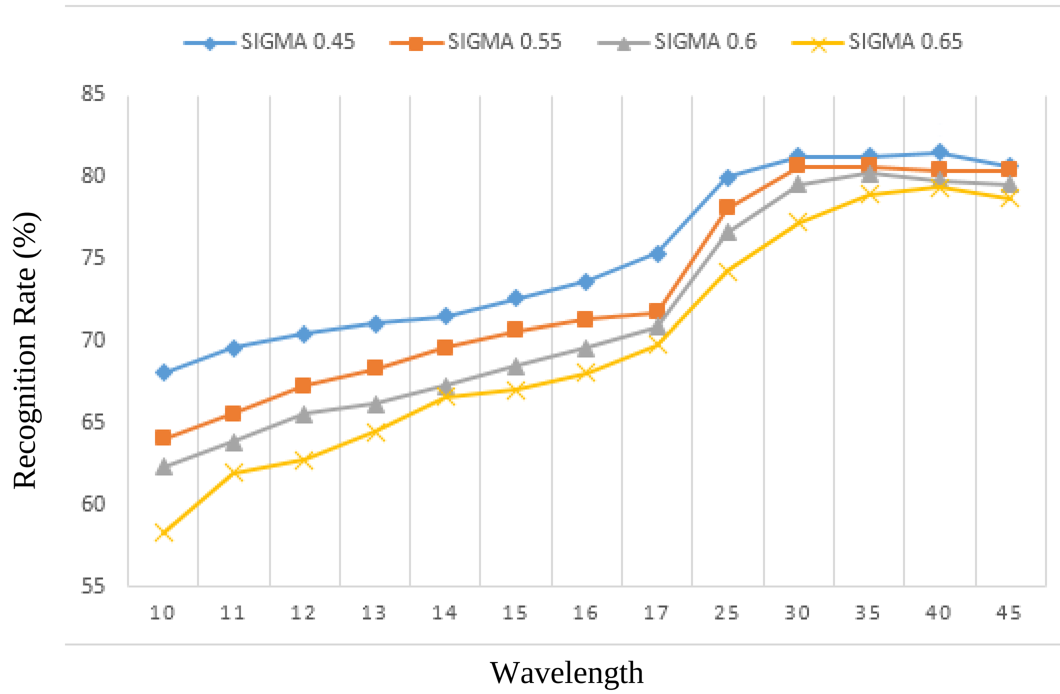

Figure 4.5: Performance Evaluation on Left Palmprint Dataset

As shown in the above tables and Figure 4.5, the best recognition rate for Log-Gabor is obtained using wavelength value as 40 and sigma value as 0.45. The best recognition rate is 81.4894% on the left palmprint dataset using Log-Gabor method.

Table 4.11: Log-Gabor Performance Evaluation for Right Hand by Using Sigma (0.45)

Experiment	Wavelength	Recognition Rate (%)
1	10	69.1489
2	11	69.7872
3	12	71.0638
4	13	72.1277
5	14	72.7660
6	15	72.7660
7	16	72.5532
8	17	72.7660
9	18	73.6170
10	20	74.8936
11	25	77.0213
12	30	77.4468
13	35	77.6596
14	40	80
15	45	79.5745
16	50	78.0851

Table 4.12: Log-Gabor Performance Evaluation for Right Hand by Using Sigma (0.55)

Experiment	**Wavelength**	**Recognition Rate (%)**
1	10	62.5532
2	11	66.5957
3	12	67.2340
4	13	68.5106
5	14	70.2128
6	15	70.8511
7	16	71.7021
8	17	71.4894
9	18	72.1277
10	20	72.9787
11	25	74.8936
12	30	76.8085
13	35	76.3830
14	40	77.4468
15	45	78.2979
16	50	78.0851

Table 4.13: Log-Gabor Performance Evaluation for Right Hand by Using Sigma (0.6)

Experiment	**Wavelength**	**Recognition Rate (%)**
1	10	59.7872
2	11	63.4043
3	12	65.5319
4	13	67.2340
5	14	68.2979
6	15	69.7872
7	16	71.0638
8	17	71.2766
9	18	71.4894
10	20	72.5532
11	25	74.4681
12	30	75.9574
13	35	76.3830
14	40	76.5957
15	45	76.1702
16	50	75.9574

Table 4.14: Log-Gabor Performance Evaluation for Right Hand by Using Sigma (0.65)

Experiment	**Wavelength**	**Recognition Rate (%)**
1	10	55.3191
2	11	59.3617
3	12	61.9149
4	13	65.3191
5	14	67.0213
6	15	68.0851
7	16	69.5745
8	17	70.2128
9	18	70.8511
10	20	71.7021
11	25	72.5532
12	30	74.8936
13	35	75.9574
14	40	76.5957
15	45	75.3191
16	50	74.2553

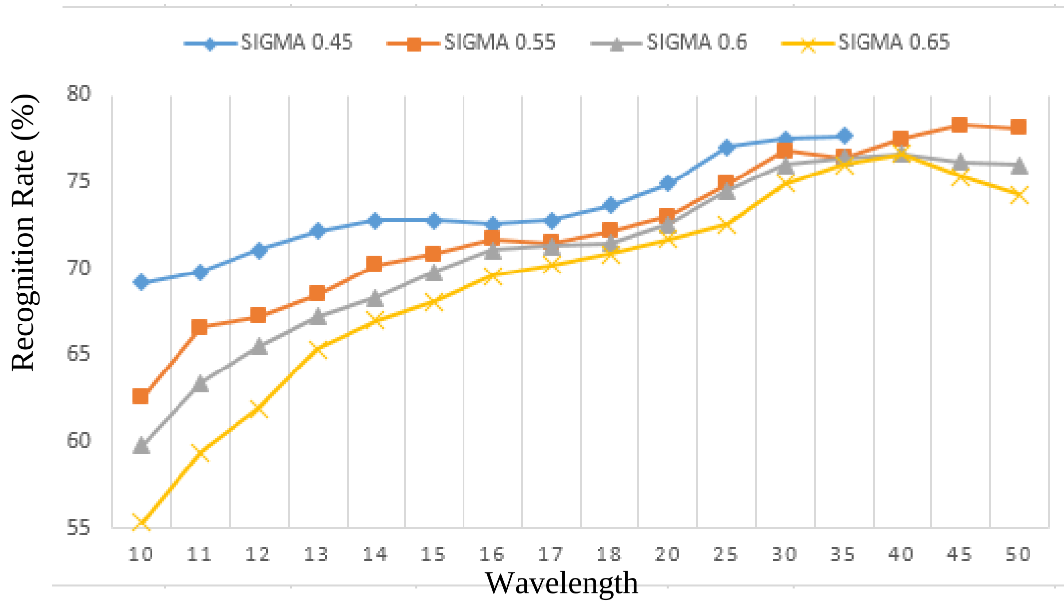

Figure 4.6: Performance Evaluation on Right Palmprint Dataset

The results presented on right palmprint dataset in the above tables and Figure 4.6, demonstrate that the best recognition rate is 80%. This value is obtained using wavelength value as 40 and sigma value as 0.45. The results achieved for palmprint recognition using both left and right hands are compatible since the best recognition rates are achieved using the same parameter values. Additionally, it can be stated that there is a small difference between left and right palmprint recognition rates.

4.3 Discussion on Experimental Results

Palmprint recognition performance using Principal Component Analysis, Discrete Cosine Transform, Local Binary Patterns and Log-Gabor is changing by using different parameter values for each algorithm. For simulations, two images for test and two for train have been used and the results showed that the best recognition performance is achieved using Local Binary Patterns method.

Local Binary Patterns method gives the highest recognition performance compared to other algorithms. The best performance with LBP for the right and left hand can be obtained when the pattern size is 12*12 for (2,8) neighborhood which gives 94.6809% for the right hand and 95.7447% for the left hand. Moreover, simulations showed that (1,8) neighborhood gives a good performance when the pattern size is 10*10, but sometimes the performance will be better than (12*12) pattern size. The results for (10*10) pattern size for the right hand are 93.4043% and the left hand 91.4894% while by using (12*12) pattern size for the right hand the accuracy becomes 93.1915% and 92.5532 % for the left hand.

The second highest performance that can be obtained for palmprint recognition is with DCT. Three different experiments have been done for evaluation. In the experiments, we have figured out the performance of DCT that is not fixed and it can be changed from one dataset to another. Moreover, by reducing the number of samples in the dataset, the performance changes. For example, in the right hand, 80.4255% can be obtained when the number of the samples in the dataset are 470. By reducing the number of train and test samples in the dataset to 300 as the number of train images and 300 as the number of test images, the performance changes to 78.3333%. Whenever the number of train and test images are decreased to 150, the performance increases to 80.6667%. The same rules apply to left hand, when the number of train/test is 470 the performance is 84.0426%. By reducing the number of samples in the dataset to 300 train/test the performance increases to 85.6667% and by taking 150 train/test the performance decreases to 83.3333%.

On the other hand, the third highest performance obtained is with Log-Gabor. The parameter values play an important role to find a good performance for this method. As shown in the previous tables, the best palmprint recognition rate can be obtained for the left hand when sigma is 0.45 and the wavelength is 40 which is 81.4894%. Similarly, the highest performance for the right hand using Log-Gabor is achieved when sigma is 0.45 and the wavelength is 40. The palmprint recognition rate in this condition is 80% which is similar to the recognition rate obtained on the left palmprint dataset.

Finally, PCA is giving the worst recognition performance compared to the other algorithms. Different experiments have been done for left and right hand. The best recognition rates using PCA approach achieved on left and right palmprint datasets are 74.6809% and 74.8926%, respectively.

Another set of experiments have been done on PCA which compares the recognition rates with different number of eigenvectors. The best performance achieved for the left hand is 75.7447% and for the right hand, it is 74.8936% when the number of eigenvectors are 380.

The best recognition rates for each method are summarized in Table 4.15 and on Figure 4.7. The comparison of PCA, DCT, Log-Gabor and LBP methods is presented for right and left palmprint datasets. The results demonstrate that LBP for both left and right hand experiments achieves the best recognition rates. The reason is that LBP is a texture-based method which is emphasizing the most important features and texture information available in palmprint images.

Table 4.15: The Best Recognition Rates for Each Method

Algorithm	**Recognition rate (%) (Right palmprint datasets)**	**Recognition rate (%) (Left palmprint datasets)**
PCA	74.8926	74.6809
DCT	80.4255	84.0426
Log-Gabor	80	81.4894
LBP	93.1915	92.5532

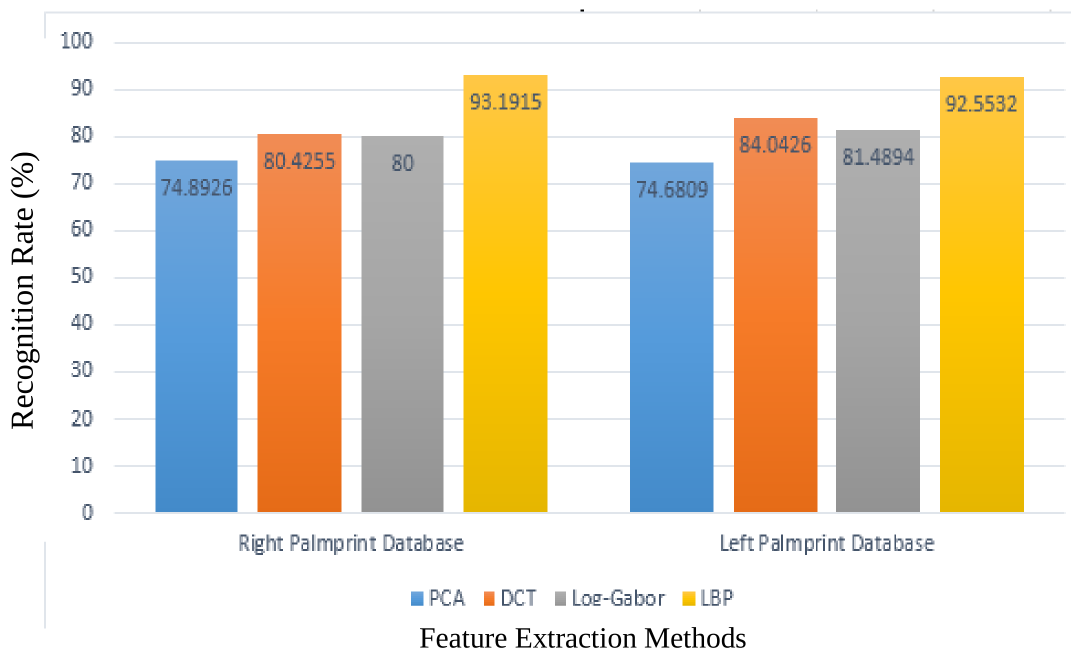

Figure 4.7: Comparative Performance Analysis on Four Methods

Chapter 5

CONCLUSION

This thesis represents a comparative study on four palmprint recognition algorithms namely Local Binary Patterns (LBP), Discrete Cosine Transform (DCT), Principal Component Analysis (PCA) and Log Gabor. All the algorithms have been investigated by using different parameters and the recognition performances have been evaluated.

For the simulations, left and right palmprint datasets of PolyU database have been used and the experimental results showed that LBP performs the best accuracy on both datasets and it has a strong ability for palmprint recognition. The reason is that LBP is a texture-based method which is emphasizing the most important features and texture information available in palmprint images.

In order to enhance the palmprint recognition performance, as a future work, a hybrid method using a combination of more than one feature extraction algorithms can be implemented. Additionally, the simulations can be repeated on other palmprint databases for the comparison of different feature extraction methods on palmprint recognition.

REFERENCES

[1] A. C. Simon, A History of Fingerprinting and Criminal Identification, Cambridge: Harvard University Press, 2002.

[2] M. Prithika and R. P, "Credit Card Duplication and Crime Prevention Using Biometrics," *IOSR Journal of Computer Engineering (IOSR-JCE),* vol. 10, no. 1, pp. 01-07, Mar. - Apr. 2013.

[3] D. Gafurov, E. Snekkenes and P. Bours, "Gait Authentication and Identification Using Wearable Accelerometer Sensor," in *IEEE*, Alghero, 2007.

[4] V. R and M. M, "Principal Component Analysis based Palmprint Recognition with Center of Mass Moments," *IJSER,* vol. 3, no. 10, pp. 1-6, october 2012.

[5] . P. P. Jayshri and N. Chhaya, "A Survey of Multispectral Palmprint Identification Techniques," *IJSET,* vol. 3, no. 8, pp. 1051-1053, August 2014.

[6] D. Zhang, W. Kong, J. You and M. Wong, "Online palmprint identification," *Pattern Analysis and Machine Intelligence, IEEE Transactions,* vol. 25, no. 9, pp. 1041-1050, September 2003.

[7] U. S. F. Government, "Biometric Center of Excellence," FBI, 2011. [Online]. Available: http://www.biometrics.gov/default.aspx.

[8] S. Tangwongsan and C. Sumetphong, "Optical Character Recognition Techniques for Restoration of Thai Historical Documents," in *2008 International Conference on Computer and Electrical Engineering*, Phuket, Thailand, 2008.

[9] B. Aleksandra , "Biometric Authentication. Types of biometric identifiers," Helsingfors, 2012.

[10] W. Kong and D. Zhang, "Palmprint texture analysis based on low-resolution images for personal authentication," in *Pattern Recognition, 2002. Proceedings. 16th International Conference*, Quebec City, Canada, 2002.

[11] L. Zhang and D. Zhang, "Characterization of palmprints by wavelet signatures via directional context modeling," *IEEE Transactions on Systems Man and Cybrentics - part B : Cybrentics*, vol. 34, no. 3, pp. 1335 - 1347, june 2004.

[12] X. Jing and D. Zhang, "A face and palmprint recognition approach based on discriminant DCT feature extraction," *IEEE Trans Syst Man Cybern B Cybern,* vol. 34, no. 6, pp. 2405-15, Dec. 2004.

[13] J. Noh and K. Rhee, "Palmprint identification algorithm using Hu invariant moments and Otsu binarization," in *Computer and Information Science, 2005. Fourth Annual ACIS,* Jeju Isl, South Korea, 2005.

[14] L. Nanni and A. Lumini , "ensemble of multiple palmprint representation," *Pergamon Elsevier Science Ltd*, vol. 36, no. 3, p. 4485–4490, April 2009.

[15] A. Kumar and D. Zhang, "Personal authentication using multiple palmprint representation," *Elsevier Sci Ltd,* vol. 38, no. 10, p. 1695 – 1704, October 2005.

[16] M. Ekinci and M. Aykut, "Palmprint recognition using kernel PCA of Gabor features," in *23'rd International Symposium on Computer and Information Sciences*, Istanbul, Turkey, 2008.

[17] M. Mu, Q. Ruan and S. Guo, "Shift and gray scale invariant features for palmprint identification using complex directional wavelet and local binary pattern," *Ecience Bv,* vol. 74, no. 17, pp. 3351-3360, October 2011.

[18] S. Linlin , W. Wenfeng and J. Sen, "Coding 3D Gabor Features for Hyperspectral Palmprint Recognition," in *2014 International Conference on Medical Biometrics*, Shenzhen, 2014.

[19] K. Pearson, "On Lines and Planes of Closest Fit to Systems of Points in Space," *Philosophical Magazine*, pp. 559-572, 1901.

[20] E. S. Paul, Summated Rating Scale Construction, California sage: Sage Publications, Inc, 1992.

[21] I. S. Lindsay, "A tutorial on Principal Component Analysis," University of Otago, Dunedin, 2002.

[22] K. R. N. A. T. Natarajan, "Discrete Cosine Transform," *IEEE Transaction on Computers*, vol. 1, pp. 90-93, 1974.

[23] R. C. G. R. Woods, Digital Image Processing Using Matlab, 3rd ed.: Prentice Hall,, 2007.

[24] L. Zhao, Y. Cai, J. Li and X. Xu, "Face recognition based on discrete cosine transform and support vector machine," in *International Conference on Neural Networks and Brain (ICNN&B 2005)*, Beijing, Peoples R China, 2005.

[25] S. Smoot and L. Rowe, "Study of DCT Coefficient Distributions," in *Conference on Human Vision and Electronic Imaging*, San Jose, CA, 1996.

[26] C. Chen, "Transform coding of digital images using variable block-size DCT with adaptive thresholding and quantization," in *Applications of Digital Image Processing XIII*, San Diego, CA, 1990.

[27] D. Omaia, . J. V. D. Poel and . L. V. Batista, "2D-DCT Distance Based Face Recognition Using a Reduced Number of Coefficients," in *22nd Brazilian Symposium on Computer Graphics and Image Processing*, Rio de Janeiro, Brazil, 2009.

[28] L. Masek, "Recognition of Human Iris Patterns for Biometric Identification," University of Western Australia, 2003.

[29] F. Mirzaei, "Age Classification using Facial Feature Extraction," Eastern Mediterranean University, Gazimagusa, 2011.

[30] S. W. James, "Death Of Sir William Herschel. Author Of Finger-Print Identity System," *Oxford University Press*, no. 41618, p. 25, Oct 25 1917.

[31] P. J. A. Shaw, Multivariate Statistics for the Environmental Sciences, 2003.

[32] M. Turk, A. Pentland, "Eigenfaces for Recognition," *Journal of Cognitive Neuroscience*, vol. 3, pp. 71-86, march 1991.

[33] A. Hervé and J. W. Lynne , "Principal Component Analysis," *Wiley Interdisciplinary Reviews: Computational Statistics*, vol. 2, no. 4, pp. 433-459, 30 JUN 2010.

[34] S. Jon , "A Tutorial on Principal Component Analysis," Cornell University, New York, 2014.

[35] D. Zhao, W. Gao and Y. Chan, "Morphological Representation of DCT Coefficients for Image Compression," *IEEE Transactions On Circuits And Systems For Video Technology*, vol. 12, no. 9, pp. 819-823, Sep 2002.

[36] J. Wu and Z. Qiu, "A Hierarchical Palmprint Identification Method Using Hand Geometry and Grayscale Distribution Features," in *18th International Conference on Pattern Recognition (ICPR 2006)*, Hong Kong, PEOPLES R CHINA, 2006.

[37] B. R. Centre, "Palmprint Database," Hong Kong Polytechnic University, 2013. [Online]. Available: http://www4.comp.polyu.edu.hk/~biometrics/MultispectralPalmprint/MSP.htm.

[38] M. Kirby and L. Sirovich, "Application of the Karhunen-Loeve Procedure for the Characterization of Human Faces," *IEEE Transactions on Pattern Analysis and Machine Intelligence*, vol. 12, no. 1, pp. 103-108, 1990.